# Chemical and Mechanical Impact of Silica Nanoparticles on the Phase Transition Behavior of Phospholipid Membranes in Theory and Experiment

C. Westerhausen,[†] F. G. Strobl,[†] R. Herrmann,[‡] A. T. Bauer,[§] S. W. Schneider,[§] A. Reller,[‡] A. Wixforth,[†] and M. F. Schneider[¶*]

[†]Experimental Physics I, Institute of Physics and Augsburg Center for Innovative Technologies and [‡]Resources Strategy, Institute of Physics, University of Augsburg, Augsburg, Germany; [§]Department of Dermatology, University Medical Center Mannheim, University of Heidelberg, Mannheim, Germany; and [¶]Biological Physics Group, Department of Mechanical Engineering, Boston University, Boston, Massachusetts

ABSTRACT The interaction of nanoparticles (NPs) with lipid membranes is an integral step in the interaction of NPs and living cells. During particle uptake, the membrane has to bend. Due to the nature of their phase diagram, the modulus of compression of these membranes can vary by more than one order of magnitude, and thus both the thermodynamic and mechanical aspects of the membrane have to be considered simultaneously. We demonstrate that silica NPs have at least two independent effects on the phase transition of phospholipid membranes: 1), a chemical effect resulting from the finite instability of the NPs in water; and 2), a mechanical effect that originates from a bending of the lipid membrane around the NPs. Here, we report on recent experiments that allowed us to clearly distinguish both effects, and present a thermodynamic model that includes the elastic energy of the membranes and correctly predicts our findings both quantitatively and qualitatively.

## INTRODUCTION

The increasing number and variety of artificially produced nanometer-scale particles calls for a thorough understanding of the influence of such nanoparticles (NPs) on biological material. In particular, many research teams are focusing on the uptake of NPs in human cells and its consequences (1,2). Silica NPs occur in exhaust emissions and are also added to food, textiles, and construction materials to improve their properties (3). Moreover, they are even considered for use in drug delivery (4). The uptake of NPs by living cells has recently become the subject of risk assessments because it correlates with cytotoxicity (5). In this context, it was shown that clathrin-dependent endocytosis is the most important pathway for the cellular uptake of silica NPs (6). For a detailed understanding of endocytotic mechanisms, it is helpful to study the mechanical properties of pure lipid membranes, which have been shown to be suitable model systems for cell membranes (7). However, one has to bear in mind that the elastic properties of the lipid membrane depend on its thermodynamic state and can vary substantially. Especially during the transition from the gel to the fluid phase, the bending modulus changes by at least one order of magnitude (8,9).

It has been demonstrated that this phase transition can trigger a variety of morphological transitions even in the absence of membrane proteins. Tube formation, fission, budding, and the expulsion of entire vesicles have been reported (10–13). Therefore, the thermodynamic state of the membrane must be considered as an important factor in the transport mechanisms of cells. The lipid phase transition can be conveniently monitored by differential scanning calorimetry (DSC), which allows one to detect even minor changes in the membrane properties (14). In 1992, Naumann et al. (15) showed that 1,2-dipalmitoyl-*sn*-glycero-3-phosphocholine (DPPC) bilayers on a spherical particle support ($R \approx 300$ nm) melted cooperatively but exhibited a suppressed pretransition. Using particles of two different sizes ($R \approx 30$ nm and $R \approx 300$ nm), Brumm et al. (16) further showed that the transition temperature of supported membranes is related to their curvature, i.e., the radius of the particles. Finally, for vesicles with diameters $<100$ nm, Ahmed and Wunder (17) applied the same concept to analyze the influence of differences in the curvatures of the inner and outer leaflets on the transition melting temperature $T_m$.

Here, we employ DSC to characterize the impact of the same NPs that have been shown to be cytotoxic for human endothelial cells (5) on different phospholipid membranes. We investigate spherical supported vesicles (SSVs) in terms of their transition temperature and find significantly different dependencies on the membrane curvature for different lipid chain lengths. To explain our experimental findings, we present a thermomechanical model that includes the bending energy of the bilayer in the thermodynamic potential. In addition, we report a chemically induced depression of $T_m$ that is triggered by the release of small amounts of silicic acid (SA) from the NPs.

## MATERIALS AND METHODS

For the experiments, we used silica particles with the following diameters: $d = 16 \pm 2$ nm, $18 \pm 2$ nm, $85 \pm 4$ nm, $212 \pm 25$ nm, $305 \pm 35$ nm, and $348 \pm 40$ nm. All NPs used were synthesized and analyzed as described previously in detail by Blechinger et al. (6). 1,2-Ditridecanoyl-*sn*-glycero-3-phosphocholine (13:0PC), 1,2-dimyristoyl-*sn*-glycero-3-phosphocholine (14:0PC), 1,2-dipentadecanoyl-*sn*-glycero-3-phosphocholine (15:0PC),

*Submitted June 27, 2011, and accepted for publication December 1, 2011.*

*Correspondence: matschnei@gmail.com

Editor: Klaus Gawrisch.



0006-3495/12/03/1032/7 $2.00

doi: 10.1016/j.bpj.2011.12.004

DPPC (16:0PC), and 1,2-diarachidoyl-*sn*-glycero-3-phosphocholine (20:0PC), dissolved in chloroform, were obtained from Avanti Polar Lipids (Alabaster, AL) and used without further purification.

Suspensions of vesicles and NPs were prepared by rehydrating a dried lipid film with a dispersion of NPs in ultrapure water (18.2 MΩcm; Pure Aqua, Tuttlingen, Germany). The final lipid concentration was 1 mg/ml. To prepare multilamellar vesicles (MLVs), the sample was heated above the main phase transition temperature $T_m$ for 60 min and vortexed several times. Afterward, the solution was either sonicated above $T_m$ for 30 min or directly loaded into the calorimeter. The pure NP dispersions as well as the SSV containing sonicated samples were analyzed regarding their colloidal stability. A dynamic light scattering analysis showed that the hydrodynamic radius of such samples did not change significantly over typical experimental timescales (i.e., several hours; see Supporting Material). Furthermore, observations of different dried samples by scanning electron microscopy/transmission electron microscopy showed no signs of large agglomerates.

The measurements were carried out with a Microcal VPDSC differential scanning calorimeter (18) at a scan rate of 17 K/h. The reference sample was ultrapure water. The supernatant of centrifuged NP dispersions was analyzed by electrospray ionization mass spectrometry (Thermo Finnigan LTQ FT, resolution 100.000 at m/z = 400, up to 2000 u, 4 kV, heating capillary temperature 250°C) to quantify the most frequent oligomers of SA released from the NPs.

## RESULTS AND DISCUSSION

### Chemical impact of silica NPs on $T_m$

When NPs were added to a suspension of MLVs, both the main transition and the pretransition peaks shifted toward lower temperatures (see Fig. 1 *A*). To quantify this effect, we analyzed the peak position of the main transition ($T_m$) as a function of particle concentration and size (Fig. 1 *B*). The mass concentration $c_m$ was chosen so as to keep the total NP surface area per sample in the same range for all NP sizes. Thus, $c_m$ covered a wider range for the larger NPs (Fig. 1 *B*).

Our experiments revealed the following trend: independently of particle size, the temperature shift of the main transition exhibits a linear dependence on the total amount of added NP mass, which indicates an effect that is not related to the total particle surface. We then repeated the measurements, substituting the particles with the supernatants of the centrifuged NP dispersions of adequate particle concentration (10,000 × *g*, 3–300 min, depending on NP size). Fig. 1 *B* shows that the temperature shift of the NP-free samples is equal to the corresponding NP-containing samples. Therefore, the shift in $T_m$ with increasing concentration is not due to the physical presence of the NPs but to substances dissolved from the NPs. This is confirmed by the fact that an increase in incubation time of washed NPs led to an increasing shift in $T_m$ as well. Alexander et al. (19) reported that silica always partially dissolves in aqueous solutions, forming SA oligomers. According to Eq. 42 of Rimstidt and Barnes (20), 95% of the equilibrium concentration of silica in water should be reached within 9 h in the case of the NPs used here. The equilibrium concentration of SA is in the range of 150 ppm (19,21). The electrospray ionization mass spectra showed that tetramers (m/z = 274.8809) and pentamers (m/z = 370.8693) are the most frequent oligomers in our NP dispersions (data not shown).

To confirm that SA is indeed the origin of the decrease in $T_m$, we added a freshly prepared and oversaturated SA solution to the MLV samples. A linear decrease in $T_m$, as presented in Fig. 2, was found.

Regarding the hydrophilic character of SA (22), we expect that headgroup effects cause the observed melting-point depression. One possible explanation could be an altered solvation of both lipid phases in an SA solution compared with water.

Disregarding the specific nature of the SA-lipid interaction, we assume that the solute SA influences the chemical potentials of gel phase $\mu_{gel}$ and fluid phase $\mu_{fluid}$

$$\mu_i(T) = \mu_i^w(T) + \Delta\mu_i^{tr}(T), \tag{1}$$

where $\mu_i^w$ denotes the standard chemical potential of the corresponding lipid phase in water, and $\mu_i^{tr}$ is the free energy associated with a transfer of the phase from water to the solution.

Along these lines, Chapman et al. (23) derived that for the shift of the transition temperature $\Delta T_m$,

$$\Delta T_m = \left[ -\frac{RT_m^2}{\Delta H(T_m)} \right] \alpha c_{SA} =: Ac_{SA}, \tag{2}$$

where $R$ is the gas constant, $T_m$ is the melting temperature of the lipid in pure water, $\Delta H(T_m)$ is the change in the system's enthalpy at $T_m$, and $c_{SA}$ is the concentration of the solute SA.

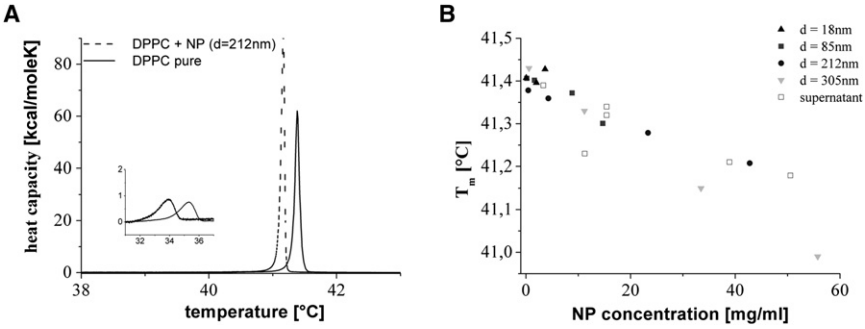


FIGURE 1 Melting-point depression due to NPs. (*A*) Heat capacity profile of an MLV sample (DPPC, 1.34 mM; *solid line*, without NPs; *dashed line*, with NPs). Inset: Pretransition region. (*B*) $T_m$ is plotted against the final mass concentration of added NPs. Different-shaped, solid symbols indicate different-sized particles. The open rectangles show the $T_m$ for NP-free samples containing only the supernatant of a centrifuged particle dispersion.

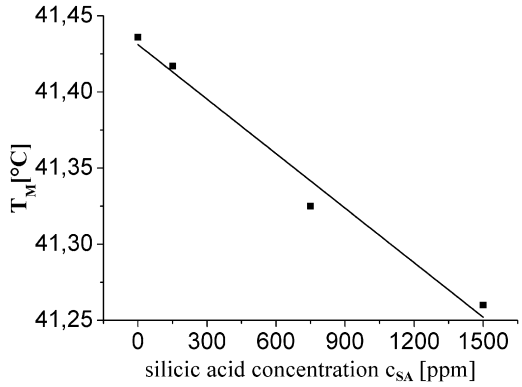


FIGURE 2 SA causes a melting-point depression. $T_m$ of DPPC MLV samples in the presence of SA. A clear linear dependence on the SA concentration can be observed.

For low concentrations $c_{SA}$ and small temperature changes, $\alpha$ is a constant that depends on the strength of the interaction of the solute with both phases, i.e., the values of $\mu^{tr}_{gel}(T_m)$ and $\mu^{tr}_{fluid}(T_m)$.

It is noteworthy that Eq. 2 should be true for a direct interaction between lipid phases and solute, as well as for indirect influences of, e.g., solvation effects. Our measurements with oversaturated SA suggest a proportionality constant of A = 0.119 mK/ppm (see Fig. 2).

We emphasize that silica NPs release small amounts of SA that can significantly influence the thermodynamic properties of lipid membranes. The concentration of dissolved SA seems to be approximately proportional to the mass concentration of NPs in the dispersion, and does not depend on their size (Fig. 1 *B*). Future studies should take this effect into account, regardless of the curvature-induced effect explained in the following section.

## Preparation of spherical solid-supported phospholipid bilayers

Storage of the samples for 1 wk after preparation led to the occurrence of an additional peak in the DSC profile at a temperature $T_s$ (see Fig. 3). After sonication, this additional peak became more pronounced than the original one at $T_m$, indicating an increasing portion of the lipids undergoing the transition at $T_s$ after this step. Some samples were centrifuged after sonication at 10,000 × *g* for 15–60 min. Before the centrifugation step was repeated, the supernatant was replaced with ultrapure water. In the inset of Fig. 3, the ratios of the transition enthalpies of the additional ($\Delta H_s$) and main ($\Delta H$) transitions are shown before and after centrifugation. Although this ratio was only ~0.01 for the untreated sample, it increased to 1 after the first centrifugation step and to 2.2 after the second step. This clearly indicates that the additional peak at $T_s$ has its origin in lipids that are attached to the NPs.

This observation and conclusion are consistent with the findings of Naumann et al. (15) and Bayerl and Bloom

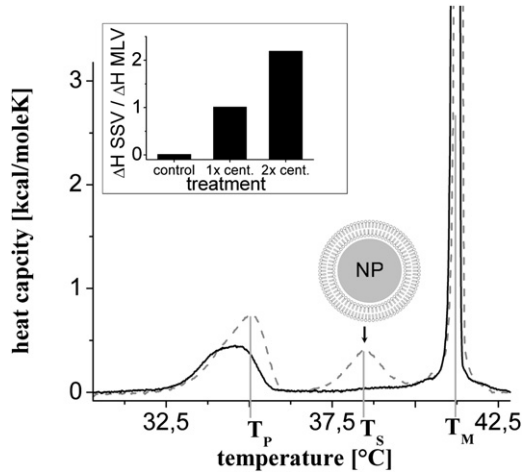


FIGURE 3 Solid support leads to an additional peak in the heat capacity profile. Heat capacity profile of a DPPC MLV sample directly after addition of NPs (*solid line*) and after 1 wk of storage at 4°C (*dashed line*). An additional peak appears (*arrow*), indicating the existence of a solid-supported lipid population. The pretransition temperature $T_p$ and main transition temperatures $T_s$ and $T_m$ for SSVs and free MLVs are indicated by vertical lines. Inset: The ratio of the enthalpies of the peak at $T_s$ and $T_m$ was determined before and after one or two centrifugation steps. With each centrifugation step, a more pronounced peak at $T_s$ verifies the assumption of a solid-supported lipid population.

(24), who coated NPs with lipid membranes and reported comparable shifts in $T_m$. Furthermore, in 1996, Brumm et al. (16) showed some differences in the curvature dependence between 14:0PC and 18:0PC; however, these authors did not perform a systematic study of the influence of NP size.

Hence, we analyzed the heat capacity profile of the supported membrane population for both NPs of different diameters (20–348 nm) and lipids with different chain lengths (13–20 carbon atoms) but identical headgroups. To account for the abovementioned chemical melting-point depression, we analyzed the difference $\Delta T := T_s - T_m$ between the transition temperatures of free and supported lipids (see Fig. 4 *A*). Assuming that the above chemical effect is of the same order for both experiments, it should cancel out.

All measurements show the same tendency, namely, a shift of $T_m$ toward lower temperatures for the solid-supported case. The heat capacity profiles for 20:0PC are shown in Fig. 4 *A* for different NP sizes. The expected broadening (15) of the SSV due to decreasing cooperativity with increasing membrane curvature was observed but not analyzed further.

Fig. 4 *B* shows $\Delta T$ for different lipids and NP diameters. Whereas $\Delta T$ decreases with decreasing NP diameter for 13:0PC, 14:0PC, and 15:0PC, it increases for 16:0PC and 20:0PC. For all lipids except 20:0PC, the limit for a flat support of zero curvature is roughly $\Delta T = -2.5$ K.

To summarize, our results consist of three main observations: 1), for all lipids and NP sizes, $T_s$ shifts toward lower temperatures, with $\Delta T$ ranging between −0.5 K

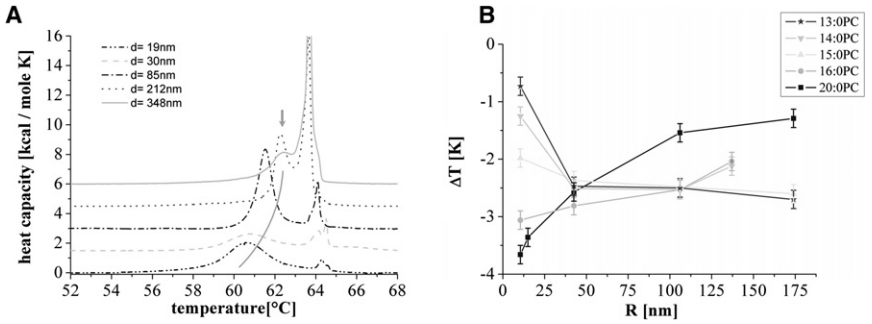


FIGURE 4 Effect of NP size and chain length. (*A*) Heat capacity profiles of 20:0PC MLV samples with silica NPs of different diameters between 19 nm and 348 nm (the baselines are shifted in the vertical direction for clarity). The gray line (*arrow*) indicates the shift in $T_s$. (*B*) The difference $\Delta T$ between $T_m$ and $T_s$ is plotted versus the NP diameter for different lipid chain lengths. The curvature dependence differs significantly.

and −4 K; 2), the curvature dependence changes its sign for increasing chain length; and 3), for all lipids, $\Delta T$ shows a saturation behavior with decreasing curvature.

## THEORY

### Bending contribution to $\Delta T$

In the case of SSVs, the vesicles spread on and covered the NPs or parts of them, and thus experienced a curved substrate. Below, we derive an analytical expression for the expected change in phase transition temperature $T_m$ based on the mechanical and calorimetric properties of the system. We therefore integrate the bending energy of the membrane in a Landau-type potential. No new or additional model assumptions are introduced; instead, we combine existing theories to provide a coherent explanation of our results.

#### *Contributions to the Landau potential*

In the Landau theory, a first-order phase transition is represented by the relative evolution of the double-well potential of the form shown in Fig. 5 (25,26):

$$\Phi(P,T,\Pi,\eta) = \Phi_0 + A\eta^2 + B\eta^4 + C\eta^6, \tag{3}$$

where $\eta$ is the order parameter and $A(T,p,\Pi)$, $B(p,\Pi)$, and $C(p,\Pi)$ are functions of the thermodynamic variables temperature $T$, bulk pressure $p$, and lateral pressure $\Pi$, respectively.

It is convenient and common to consider only the evolution of the potential minima in $\eta$ with temperature. These minima are commonly identified with the Gibbs free-energy potentials for the gel phase and fluid phase (27,28), as indicated in Fig. 6.

In the absence of any solid support, the two potentials intersect at the phase transition temperature $T_m$ (see Fig. 6). The additional energies $\Delta G_{gel}$ and $\Delta G_{fluid}$ (see Fig. 5) in the presence of the support shifts the intersection toward lower temperatures $T_s$. For the transition temperature $T_s$ now holds:

$$G_{gel}(T_S) + \Delta G_{gel} = G_{fluid}(T_S) + \Delta G_{fluid}. \tag{4}$$

Assuming the pressure $p$ to be constant and $\partial^2\pi/\partial T^2 \approx 0$, as shown previously (29), $G_{gel}(T)$ and $G_{fluid}(T)$ can be approximated by a first-order Taylor series near the transition point $T_m$:

$$\begin{aligned} &G_{gel}(T_m) + \frac{\partial G_{gel}}{\partial T}\bigg|T_m(T_s - T_m) \; + \Delta G_{gel} \\ &\quad = G_{gel}(T_m) + \frac{\partial G_{fluid}}{\partial T}\bigg|T_m(T_s - T_m) + \Delta G_{fluid} \end{aligned} \tag{5}$$

and consequently

$$\begin{aligned} \Delta T: \; = T_s - T_m &= -\frac{\Delta G_{gel} - \Delta G_{fluid}}{\left(\frac{\partial G_{gel}}{\partial T}\bigg|T_m - \frac{\partial G_{fluid}}{\partial T}\bigg|T_m\right)} \\ &=: -\frac{\Delta G_{gel} - \Delta G_{fluid}}{\Delta\left(\frac{\partial G}{\partial T}\right)}. \end{aligned} \tag{6}$$

This general analytical expression relates the contribution of the solid support to the free energy $\Delta G_{gel/fluid}$ with the shift of the transition temperature $\Delta T$.

#### *$\Delta\,\partial G/\partial T$ from the heat capacity profile*

$\Delta\,\partial G/\partial T$ can be extracted from the experimental DSC data, recalling the relation between the thermodynamic potential $G$ and the heat capacity $c_p$ as its susceptibility:

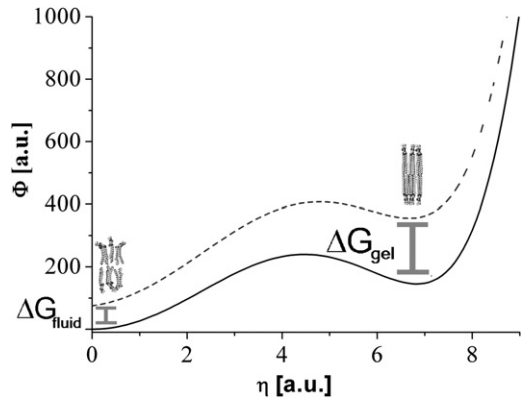


FIGURE 5 Landau representation of the thermodynamic potential. The presence of the solid support (NP) can be represented as an additional thermodynamic force (mechanical stress) on the membrane that causes a relative shift (*dashed line*) of the lower symmetry versus the higher symmetry phase minimum.

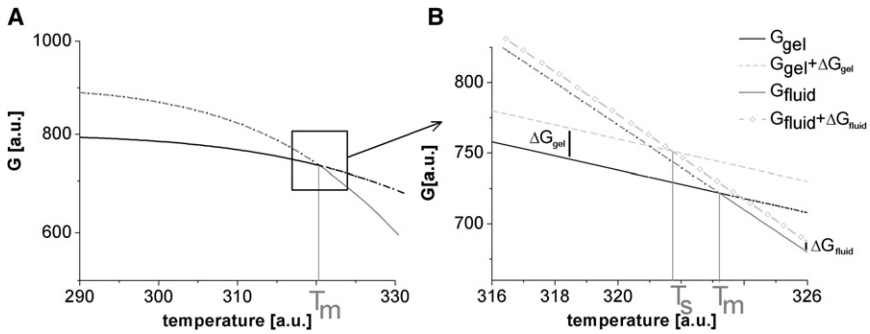


FIGURE 6 Minimum of Gibbs free-energy representation of the main transition. (*A*) The phase transition takes place at the intersection ($T_m$) of the potentials of both phases (*black line*, gel phase; *gray line*, fluid phase). (*B*) Linear approximation of $G$ near $T_m$. The dark line is the Gibbs free energy $G$ of the gel phase without solid support $G_{gel}$, the dashed line is $G_{gel}(T)$ shifted by the contribution $\Delta G_{gel}$ due to the support, the gray solid line is the potential of the fluid phase $\Delta G_{fluid}(T)$, and the dashed-dotted line is $\Delta G_{fluid}(T)$ shifted by the contribution $\Delta G_{fluid}$ due to the support. The resulting phase transition is now taking place at a lower temperature $T_s$ at the intersection of the dashed and dashed-dotted lines.

$$-T\frac{\partial^2 G}{\partial T^2}\Big|_p = T\frac{\partial S}{\partial T}\Big|_p = c_p \tag{7}$$

In agreement with the linear approximation that was described above, we have to integrate over $\partial^2 G/\partial T^2$ (respectively $c_p$) in the transition region to get $\Delta\ \partial G/\partial T$:

$$\Delta\frac{\partial \boldsymbol{G}}{\partial \boldsymbol{T}} = \int_{T_1}^{T_2}\frac{\partial^2 G}{\partial T^2}dT = -\int_{T_1}^{T_2}\frac{\boldsymbol{c_p}}{\boldsymbol{T}}\mathbf{dT} \approx -\frac{\Delta \mathrm{H}}{T_m} \tag{8}$$

The last approximation introduces the transition enthalpy $\Delta H$ and holds for sharp transitions for which a constant temperature $T_m$ can safely be assumed.

### *Mechanical contributions to ΔG*

In the case of SSVs, we consider two main contributions to $\Delta G$: 1), a curvature-dependent one caused by the bending of the membrane; and 2), a curvature-independent one due to the bare presence of the substrate (planar limit). The latter, constant contribution to $\Delta G$ can be caused by various interactions between lipids and support, for example by electrostatic forces.

To describe the mechanical contribution due to curvature, we use the well-known expression for the bending energy $E_{bend}$ of a membrane (30). For the curvature-independent contribution, we add an additional constant $G_s$:

$$\Delta \mathrm{G} = E_{bend} + G_s \approx \frac{1}{2}\left(\frac{2}{R} - \frac{1}{R_0}\right)^2 \kappa A_{mem} + \frac{1}{R^2}\kappa_G A_{mem} + G_s, \tag{9}$$

where $A_{mem}$ is the area of one lipid molecule, $c_0 := 1/R_0$ is the spontaneous curvature, $\kappa$ is the bending modulus, and $\kappa_G$ is the modulus of Gaussian curvature. In the case of a chemically symmetric bilayer, the spontaneous curvature is caused by the asymmetry of the environment due to the NP and a thin layer of water inside and the bulk water outside the vesicle. The bending radius $R$ is simply determined by the radius $R$ of the particle.

Due to the higher flexibility of lipid membranes in the fluid phase, we assume a stronger contribution of the mechanical bending energy to $\Phi$ for the low symmetric gel phase (Fig. 5.). Therefore, we neglect the bending energy contribution to $\Delta G_{fluid}$. The final expression for the temperature shift $\Delta T$ can then be found by combining Eqs. 6, 8, and 9:

$$\begin{aligned}\Delta T &= -T_m\frac{\frac{1}{2}\left(\frac{2}{R}-\frac{1}{R_0}\right)^2\kappa A_{mem}+\frac{1}{R^2}\kappa_G A_{mem}+G_{S\ gel}-G_{S\ fluid}}{\Delta H}\ \underline{\underline{\mathrm{def}}}\\ &= -T_m\frac{\frac{1}{2}\left(\frac{2}{R}-\frac{1}{R_0}\right)^2\kappa A_{mem}+\frac{1}{R^2}\kappa_G A_{mem}+\Delta G_s}{\Delta H},\end{aligned} \tag{10}$$

where $\kappa$ and $\kappa_G$ are the mechanical parameters for the gel phase and $\Delta G_s := G_{Sgel} - G_{Sfluid}$.

This expression explicitly relates the shift $\Delta T$ of the main phase transition temperature with the mechanical and calorimetric properties of the membrane, and predicts trends that can be compared with the experiments.

## DISCUSSION

In Fig. 7 we show that our thermodynamic model can well explain the observed trends of the temperature shift for different lipid chain lengths. Equation 10 was fitted to the data points of Fig. 4 *B*. $T_m$ and $\Delta H$ were taken from the heat capacity profiles, and $k$ was set to 2.5 $10^{-18}$J for 16:0PC and estimated according to $\kappa = 2.5\ 10^{-18}\mathrm{J}(h/16)^3$ for the other lipids, where $h$ is the number of carbon atoms of the hydrophobic chains of the lipids (31,32). Furthermore, $A_{mem}$ was set as 0.5 nm$^2$ and $R$ is the radius of the NPs. Thus there are three unknown parameters: $\Delta G_s$, $\kappa_G$, and $1/R_0$. We will show that $\kappa_G$ turns out to be the crucial parameter.

Initially we perform a three-parameter fit ($\Delta G_s$, $R_0$, and $\kappa_G$ free) to obtain a first estimate of the magnitude of the free parameters (Fig. S3 *a*). Because $\Delta G_s$ denotes a mainly headgroup-associated energy contribution, it is reasonable to consider $\Delta G_s$ as constant. Consistent fits are achieved for $\Delta G_s$ = constant = 150 J/mol. The two-parameter fit

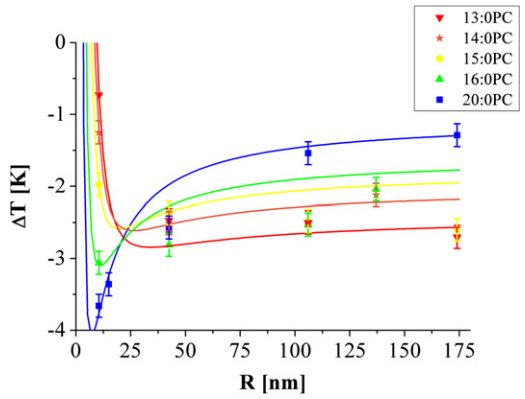


FIGURE 7 One-parameter fit of the model (Eq. 10) to the data points of Fig. 4 *B* ($\Delta G_s = 140$ J/mol, $R_0 = -250$ nm).

with fixed $\Delta G_s$ still shows good qualitative and quantitative agreement between the theory (Eq. 10) and experiments (Fig. S3 *b*). The values for $R_0$ and $\kappa_G$ are comparable to those of the three-parameter fit mentioned before (Fig. S3 *c*).

Because the fit parameters affect each other, we also compare the aforesaid results with a one-parameter fit by additionally keeping $R_0$ fixed ($\Delta G_s = 140$ J/mol, $R_0 = -250$ nm). We still achieve very good agreement between the measurements and the analytical curves from Eq. 10 (Fig. 7).

For all fits. the ratio $z := \kappa_G/\kappa$ is a critical parameter, which turns out to be roughly $-2$ for all experiments. Independently of $\Delta G_s$ and $R_0$, any substantial deviation from $-2$ would predict transition temperature shifts $\Delta T$ more than an order of magnitude larger than the ones observed. Our model therefore delivers the ratio $z$ as predicted by Helfrich (33) for the transition regime from the lamellar to the vesicular phase.

Finally, we note that in fits with $R_0$ as a free parameter and fixed $z$, a contradiction with earlier theoretical work (33,34) appears. Instead of a decrease in the spontaneous curvature $1/R_0$ with increasing $h$, as theoretically predicted, the fit indicates an increase. We hope that a more thorough understanding of $\Delta G_s$, as well as better models and more information than is currently available for $R_0$, will improve the model in the near future. Along the same lines, a refined model would account for more subtle differences in bending energy between fluid and gel phases, and consider variations in $A_{mem}$.

## CONCLUSION

In summary, our in-depth theoretical and experimental studies of the NP-membrane interaction show that silica NPs are able to influence the thermodynamic state of lipid membranes via at least two different mechanisms. First, we clearly identified a melting-point depression caused by SA released from the NPs in aqueous solution, which highlights the need for a thorough analysis of the chemical stability of NPs before studies on their interaction with biological matter. Even minute amounts of soluble substances can significantly change the thermodynamic properties of lipid membranes. Apart from this chemical aspect, we also found a size-dependent impact of silica NPs on the thermodynamic properties of phospholipid membranes mediated by the bending energy of the membrane. We propose an analytical expression that describes the shift in $T_s$ of solid-supported lipid bilayers by means of thermodynamic and mechanical considerations. Together with further experimental data, this could offer a way to estimate the modulus of Gaussian curvature of lipid membranes, a parameter that is very difficult to access otherwise. Finally, we note that previous studies have shown that ion permeability, morphological changes, and adhesion phenomena can be controlled by a shift in the thermodynamic state of the lipid membranes (11,12,27,35). A comparison between these data and the shift in state by NPs observed here demonstrates that, in principle, NPs are capable of inducing such phenomena. We believe that similar changes in membrane state may be induced in the membranes of cells. In experiments conducted in collaboration with Bauer et al. (5), we showed that the same NPs studied here increase their toxicity with total surface area and not simply with mass, which clearly exemplifies the role of NP-cell membrane contact. It will be interesting to determine the extent to which this contact modifies the thermodynamic state of the cell membrane.

## SUPPORTING MATERIAL

Three figures are available at http://www.biophysj.org/biophysj/supplemental/S0006-3495(11)05370-7.

We thank our collaborative group headed by Prof. C. Bräuchle, Ludwig Maximilians Universität, Munich, for the mass spectroscopy measurements.

This work was financially supported by the Nanosystems Initiative Munich and the Deutsche Forschungsgemeinschaft through SPP1313 BIOMEM (to A.R., M.F.S., S.W.S., and A.W.).

## REFERENCES

1. Greulich, C., S. Kittler, …, M. Köller. 2009. Studies on the biocompatibility and the interaction of silver nanoparticles with human mesenchymal stem cells (hMSCs). *Langenbecks Arch. Surg.* 394:495–502.
2. Rothen-Rutishauser, B., R. N. Grass, …, W. J. Stark. 2009. Direct combination of nanoparticle fabrication and exposure to lung cell cultures in a closed setup as a method to simulate accidental nanoparticle exposure of humans. *Environ. Sci. Technol.* 43:2634–2640.
3. Knauer, S. K., and R. H. Stauber. 2009. Controversy at the nanohype: nanoparticle–friend or enemy? *DZKF.* 5–6, 20–26.
4. Barbé, C., J. Bartlett, …, G. Calleja. 2004. Silica particles: a novel drug-delivery system. *Adv. Mater.* 16:1959–1966.
5. Bauer, A. T., E. Strozyk, …, S. W. Schneider. 2011. Cytotoxicity of silica nanoparticles through exocytosis of von Willebrand factor and necrotic cell death in primary human endothelial cells. *Biomaterials.* 32:8385–8393.

6. Blechinger, J., R. Herrmann, …, C. Bräuchle. 2010. Perylene-labeled silica nanoparticles: synthesis and characterization of three novel silica nanoparticle species for live-cell imaging. *Small.* 6:2427–2435.
7. Simons, K., and W. L. C. Vaz. 2004. Model systems, lipid rafts, and cell membranes. *Annu. Rev. Biophys. Biomol. Struct.* 33:269–295.
8. Heimburg, T. 2007. Thermal Biophysics of Membranes. Wiley-VCH Verlag GmbH & Co. KGaA, Weinheim, Germany.
9. Kwok, R., and E. Evans. 1981. Thermoelasticity of large lecithin bilayer vesicles. *Biophys. J.* 35:637–652.
10. Roux, A., D. Cuvelier, …, B. Goud. 2005. Role of curvature and phase transition in lipid sorting and fission of membrane tubules. *EMBO J.* 24:1537–1545.
11. Leirer, C., B. Wunderlich, …, M. F. Schneider. 2009. Phase transition induced fission in lipid vesicles. *Biophys. Chem.* 143:106–109.
12. Franke, T., C. T. Leirer, …, M. F. Schneider. 2009. Phase-transition- and dissipation-driven budding in lipid vesicles. *ChemPhysChem.* 10:2852–2857.
13. Leirer, C. T., B. Wunderlich, …, M. F. Schneider. 2009. Thermodynamic relaxation drives expulsion in giant unilamellar vesicles. *Phys. Biol.* 6:016011.
14. Seelig, J. 2004. Thermodynamics of lipid-peptide interactions. *Biochim. Biophys. Acta.* 1666:40–50.
15. Naumann, C., T. Brumm, and T. M. Bayerl. 1992. Phase transition behavior of single phosphatidylcholine bilayers on a solid spherical support studied by DSC, NMR and FT-IR. *Biophys. J.* 63:1314–1319.
16. Brumm, T., K. Jørgensen, …, T. M. Bayerl. 1996. The effect of increasing membrane curvature on the phase transition and mixing behavior of a dimyristoyl-*sn*-glycero-3-phosphatidylcholine/ distearoyl-*sn*-glycero-3-phosphatidylcholine lipid mixture as studied by Fourier transform infrared spectroscopy and differential scanning calorimetry. *Biophys. J.* 70:1373–1379.
17. Ahmed, S., and S. L. Wunder. 2009. Effect of high surface curvature on the main phase transition of supported phospholipid bilayers on SiO2 nanoparticles. *Langmuir.* 25:3682–3691.
18. Plotnikov, V. V., J. M. Brandts, …, J. F. Brandts. 1997. A new ultrasensitive scanning calorimeter. *Anal. Biochem.* 250:237–244.
19. Alexander, G. B., W. M. Heston, and R. K. Iler. 1954. The solubility of amorphous silica in water. *J. Phys. Chem.* 58:453–455.
20. Rimstidt, J. D., and H. L. Barnes. 1980. The kinetics of silica-water reactions. *Geochim. Cosmochim. Acta.* 44:1683–1699.
21. O'Connor, T. L., and S. A. Greenberg. 1958. The kinetics for the solution of silica in aqueous solutions. *J. Phys. Chem.* 62:1195–1198.
22. Iler, R. K. 1979. The Chemistry of Silica. John Wiley & Sons, New York.
23. Chapman, D., W. E. Peel, …, T. H. Lilley. 1977. Lipid phase transitions in model biomembranes. The effect of ions on phosphatidylcholine bilayers. *Biochim. Biophys. Acta.* 464:260–275.
24. Bayerl, T. M., and M. Bloom. 1990. Physical properties of single phospholipid bilayers adsorbed to micro glass beads. A new vesicular model system studied by 2H-nuclear magnetic resonance. *Biophys. J.* 58:357–362.
25. Landau, L. D. 1987. Statistische Physik. Akademie Verlag, Berlin.
26. Callen, H. 1985. Thermodynamics and an Introduction to Thermostatistics, 2nd ed. Wiley-VCH, Weinheim, Germany.
27. Schneider, M. F., D. Marsh, …, T. Heimburg. 1999. Network formation of lipid membranes: triggering structural transitions by chain melting. *Proc. Natl. Acad. Sci. USA.* 96:14312–14317.
28. Tyäuble, H., M. Teubner, …, H. Eibl. 1976. Electrostatic interactions at charged lipid membranes. I. Effects of pH and univalent cations on membrane structure. *Biophys. Chem.* 4:319–342.
29. Steppich, D., J. Griesbauer, …, M. F. Schneider. 2010. Thermomechanic-electrical coupling in phospholipid monolayers near the critical point. *Phys. Rev. E.* 81:061123.
30. Helfrich, W. 1973. Elastic properties of lipid bilayers: theory and possible experiments. *Z. Naturforsch. C.* 28:693–703.
31. Seto, H., N. L. Yamada, …, T. Takeda. 2008. Bending modulus of lipid bilayers in a liquid-crystalline phase including an anomalous swelling regime estimated by neutron spin echo experiments. *Eur Phys J E Soft Matter.* 26:217–223.
32. Marsh, D. 2006. Elastic curvature constants of lipid monolayers and bilayers. *Chem. Phys. Lipids.* 144:146–159.
33. Helfrich, W. 1981. Amphophilic mesophases made of defects. *In* Physics of Defects. R. Balian, M. Kleman, and J.-P. Poirier, editors.; North Holland, Amsterdam.
34. Winterhalter, M., and W. Helfrich. 1988. Effect of surface charge on the curvature elasticity of membranes. *J. Phys. Chem.* 92:6865–6867.
35. Wunderlich, B., C. Leirer, …, M. F. Schneider. 2009. Phase-state dependent current fluctuations in pure lipid membranes. *Biophys. J.* 96:4592–4597.